

# Evolution of the Obliquities of the Giant Planets in Encounters during Migration

Man Hoi Lee <sup>a</sup>, S. J. Peale <sup>a</sup>, Eric Pfahl <sup>b</sup>, William R. Ward <sup>c</sup>

<sup>a</sup> *Department of Physics, University of California, Santa Barbara, CA 93106*

<sup>b</sup> *Kavli Institute for Theoretical Physics, University of California, Santa Barbara, CA 93106*

<sup>c</sup> *Space Studies Department, Southwest Research Institute, Boulder, CO 80302*

## ABSTRACT

Tsiganis et al. [Tsiganis, K., et al., 2005. *Nature* 435, 459–461] have proposed that the current orbital architecture of the outer solar system could have been established if it was initially compact and Jupiter and Saturn crossed the 2:1 orbital resonance by divergent migration. The crossing led to close encounters among the giant planets, but the orbital eccentricities and inclinations were damped to their current values by interactions with planetesimals. Brunini [Brunini, A., 2006. *Nature* 440, 1163–1165] has presented widely publicized numerical results showing that the close encounters led to the current obliquities of the giant planets. We present a simple analytic argument which shows that the change in the spin direction of a planet relative to an inertial frame during an encounter between the planets is very small and that the change in the obliquity (which is measured from the orbit normal) is due to the change in the orbital inclination. Since the inclinations are damped by planetesimal interactions on timescales much shorter than the timescales on which the spins precess due to the torques from the Sun, especially for Uranus and Neptune, the obliquities should return to small values if they are small before the encounters. We have performed simulations using the symplectic integrator SyMBA, modified to include spin evolution due to the torques from the Sun and mutual planetary interactions. Our numerical results are consistent with the analytic argument for no significant remnant obliquities.

## 1. INTRODUCTION

One of the fundamental questions of solar system formation is the origin of planetary spins. The spin axes of three of the four giant planets in our solar system are tilted significantly, with the present values of the obliquities (the angle between the spin axis and the orbit normal) of Jupiter, Saturn, Uranus, and Neptune equal to  $3^\circ$ ,  $27^\circ$ ,  $98^\circ$ , and  $30^\circ$ , respectively. Brunini (2006a) has recently proposed a unified mechanism for the origin of the obliquities of the giant planets. The starting point of Brunini's model is the so-called Nice model (Tsiganis et al. 2005) for the establishment of the orbital architecture of the giant planets. In the Nice model, the outer solar system was

initially compact, with Jupiter and Saturn closer than their mutual 2:1 mean-motion resonance and all of the giant planets within  $\sim 18$  AU of the Sun. The scattering of planetesimals initially in a disk starting just beyond the orbits of the planets caused Jupiter to migrate inward and Saturn, Uranus, and Neptune outward. When Jupiter and Saturn crossed the 2:1 mean-motion resonance, their orbital eccentricities were excited and the orbits of Uranus and Neptune were destabilized. A phase of close encounters among the giant planets followed, and Uranus and Neptune were scattered outward. The orbital eccentricities and inclinations of the giant planets were eventually damped to their present values by the interactions with planetesimals. Brunini (2006a) has performed numerical simulations of the Nice model that follow the evolution of the planetary spin axes. He found that large obliquities are generated during the encounter phase and that the final obliquities are similar to the present values, including the  $98^\circ$  obliquity of Uranus.

Brunini (2006b) has subsequently retracted his paper on the basis that simulations performed with another numerical code do not reproduce the previous results and show changes in the obliquities of only a few degrees in most runs. However, he did not provide any physical explanation as to why the later numerical results are more likely to be correct. Given the wide publicity of the first results, we thought it important to show in this paper a simple analytic argument (Section 2) that explains why significant obliquities of the outer planets cannot result from close encounters between these planets in the Nice model. The analytic argument is verified by numerical simulations (Section 3). We note that a summary of our results was presented by Lee et al. (2006) prior to the retraction by Brunini (2006b). While our focus is on the Nice model, our analysis of the obliquity changes in encounters can also be adapted to any scenario involving close encounters among the planets, such as the scenario proposed by Goldreich et al. (2004, see also Chiang et al. 2006), in which several ice giants were formed in the outer solar system and all but two were ejected by encounters.

## 2. ANALYTIC ARGUMENT

Let us consider the change in the spin direction of a planet of mass  $M$ , radius  $R$ , and spin frequency  $\omega$ , due to an encounter with a perturbing planet of mass  $M_{\text{pert}}$ . If we assume principle axis rotation, the spin angular momentum of the planet is

$$\mathbf{L} = (\lambda + \ell)MR^2\omega\mathbf{s}, \quad (1)$$

and the torque from the perturber at a distance  $r$  in the direction  $\hat{\mathbf{r}}$  is

$$\mathbf{N} = 3\frac{GM_{\text{pert}}}{r^3}(J_2 + q')MR^2(\hat{\mathbf{r}} \cdot \mathbf{s})(\hat{\mathbf{r}} \times \mathbf{s}), \quad (2)$$

where  $\mathbf{s}$  is the unit vector of the spin direction,  $\lambda$  is the moment of inertia of the planet normalized to  $MR^2$ , and  $J_2$  is the quadrupole coefficient of the planet. The torque from the planet's oblate figure on a satellite locks the satellite to the planet's equator plane if the nodal precession period of

the satellite is short compared to the timescale on which the spin direction of the planet is changed (Goldreich 1965). In the above equations,  $\ell$  is the orbital angular momentum (normalized to  $MR^2\omega$ ) of the satellites whose orbits are coupled to the planet's equator, and  $q'/J_2$  is the ratio of the torque from the perturber on the satellites to that directly exerted on the planet (see Ward and Hamilton 2004 for explicit definitions of  $\ell$  and  $q'$ ). From  $d\mathbf{L}/dt = \mathbf{N}$ , the rate of change of the spin direction is

$$\frac{d\mathbf{s}}{dt} = 2\alpha \left( \frac{M_{\text{pert}}}{M_0} \right) \left( \frac{A}{r} \right)^3 (\hat{\mathbf{r}} \cdot \mathbf{s})(\hat{\mathbf{r}} \times \mathbf{s}), \quad (3)$$

where  $M_0$  is the mass of the Sun and

$$\alpha = \frac{3GM_0}{2\omega A^3} \left( \frac{J_2 + q'}{\lambda + \ell} \right) \quad (4)$$

is the precession constant of the planet (plus its satellites) at the *current* orbital semimajor axis,  $A$ , of the planet.

Because the torque decreases rapidly with the distance  $r$ , we expect the total change in the spin direction in an encounter,  $|\Delta\mathbf{s}|$ , to be roughly equal to the rate of change at closest approach,  $|d\mathbf{s}/dt|_{r_p}$ , times the duration of closest approach,  $r_p/v_p$ :

$$|\Delta\mathbf{s}| \sim \left| \frac{d\mathbf{s}}{dt} \right|_{r_p} \frac{r_p}{v_p} \propto \alpha \left( \frac{M_{\text{pert}}}{M_0} \right) \left( \frac{A}{r_p} \right)^2 \frac{A}{v_p}, \quad (5)$$

where  $r_p$  and  $v_p$  are, respectively, the relative separation and speed at closest approach and the proportionality constant is a function of the encounter geometry. A more accurate expression for  $\Delta\mathbf{s}$  can be obtained by neglecting solar gravity and using the two-body approximation during the encounter. Then

$$\Delta\mathbf{s} = \int_{-\infty}^{+\infty} \frac{d\mathbf{s}}{dt} dt = \int_{-\arccos(-1/e)}^{+\arccos(-1/e)} \frac{d\mathbf{s}}{dt} \left( \frac{df}{dt} \right)^{-1} df, \quad (6)$$

where  $e(\geq 1)$  and  $f$  are, respectively, the eccentricity and true anomaly of the relative orbit. In the coordinate system where the relative orbit is in the  $x$ - $y$  plane and the closest approach is in the  $x$  direction, the integration in Eq. (6) yields

$$\begin{aligned} \Delta\mathbf{s} = & \alpha \left( \frac{M_{\text{pert}}}{M_0} \right) \left( \frac{A}{r_p} \right)^2 \frac{A}{v_p} \frac{1}{1+e} \\ & \times \left\{ \left[ \arccos(-1/e) + \frac{e}{3} (2 + 1/e^2) (1 - 1/e^2)^{1/2} \right] \sin 2\theta \sin \phi \hat{\mathbf{x}} \right. \\ & \quad - \left[ \arccos(-1/e) + \frac{e}{3} (4 - 1/e^2) (1 - 1/e^2)^{1/2} \right] \sin 2\theta \cos \phi \hat{\mathbf{y}} \\ & \quad \left. + \frac{2e}{3} (1 - 1/e^2)^{3/2} \sin^2 \theta \sin 2\phi \hat{\mathbf{z}} \right\}, \quad (7) \end{aligned}$$

where  $\theta$  and  $\phi$  are the spherical coordinate angles specifying the orientation of the spin axis in the  $xyz$  system:  $\mathbf{s} = \sin \theta \cos \phi \hat{\mathbf{x}} + \sin \theta \sin \phi \hat{\mathbf{y}} + \cos \theta \hat{\mathbf{z}}$ . Contour plots of the magnitude,  $|\Delta\mathbf{s}|$ ,

as a function of  $\theta$  and  $\phi$  show that  $|\Delta \mathbf{s}|$  reaches equal maximum values at four points with  $\theta = 45^\circ$  or  $135^\circ$  and  $\phi = 0^\circ$  or  $180^\circ$  for any  $e > 1$ . For  $e = 1$  (i.e., parabolic encounter),  $|\Delta \mathbf{s}| = (\pi/2)\alpha(M_{\text{pert}}/M_0)(A/r_p)^2(A/v_p)|\sin 2\theta|$ , which is independent of  $\phi$  and maximum at  $\theta = 45^\circ$  or  $135^\circ$ . The plot of the maximum  $|\Delta \mathbf{s}|$  for a given  $e$  as a function of  $e$  shows that it decreases monotonically with increasing  $e$ . Thus  $|\Delta \mathbf{s}|$ , as a function of  $e$ ,  $\theta$ , and  $\phi$ , is maximum for  $e = 1$  and  $\theta = 45^\circ$  or  $135^\circ$ :

$$|\Delta \mathbf{s}|_{\text{max}} = \frac{\pi}{2}\alpha \left( \frac{M_{\text{pert}}}{M_0} \right) \left( \frac{A}{r_p} \right)^2 \frac{A}{v_p}. \quad (8)$$

Since Uranus has the largest current obliquity and the largest changes in its spin direction come from encounters with Saturn, we consider first the change in the spin direction of Uranus due to an encounter with Saturn. As we shall see in Figs. 1 and 2, Saturn’s orbit (of semimajor axis  $a_S$ ) remains nearly circular, and an encounter between Saturn and Uranus must have Uranus on an eccentric orbit (of eccentricity  $e_U$ ), with Uranus usually near its perihelion. Thus the relative encounter speed at large separation is  $v_0 \approx (GM_0/a_S)^{1/2}[(1 + e_U)^{1/2} - 1] \lesssim 0.22(GM_0/a_S)^{1/2}$  if  $e_U \lesssim 0.5$ . Since the encounter phase occurs long after the formation of the regular satellites in the Nice model, the regular satellite systems must survive the encounter, and a reasonable lower limit to the separation  $r_p$  at closest approach is the semimajor axis  $a_{\text{Titan}}$  of the orbit of Titan around Saturn. For  $r_p = a_{\text{Titan}}$ ,  $2G(M_S + M_U)/r_p \gg v_0^2$  (where  $M_S$  and  $M_U$  are the masses of Saturn and Uranus, respectively), and  $v_p = [v_0^2 + 2G(M_S + M_U)/r_p]^{1/2} \approx [2G(M_S + M_U)/r_p]^{1/2}$ . So the maximum change in the spin direction of Uranus from an encounter with Saturn is

$$|\Delta \mathbf{s}|_{\text{max,U}}^S = 0.33(a_{\text{Titan}}/r_p)^{3/2}, \quad (9)$$

if we adopt  $\alpha_U = (4.6 \text{ Myr})^{-1}$  from Tremaine (1991).

For the same encounter between Uranus and Saturn, the maximum change in the spin direction of Saturn is  $|\Delta \mathbf{s}|_{\text{max,S}}^U = 0.11(a_{\text{Titan}}/r_p)^{3/2}$  if  $\alpha_S = (0.26 \text{ Myr})^{-1}$  (Tremaine 1991). If we also adopt  $\alpha_N = (17.6 \text{ Myr})^{-1}$  from Tremaine (1991), the changes from an encounter between Neptune and Saturn are nearly identical to those from an encounter between Uranus and Saturn, with  $|\Delta \mathbf{s}|_{\text{max,N}}^S \approx |\Delta \mathbf{s}|_{\text{max,U}}^S$  and  $|\Delta \mathbf{s}|_{\text{max,S}}^N \approx |\Delta \mathbf{s}|_{\text{max,S}}^U$ , because Uranus and Neptune have similar masses and  $\alpha_U A_U^3 \approx \alpha_N A_N^3$  (see Eq. (8)). For an encounter between Uranus and Neptune,  $|\Delta \mathbf{s}|_{\text{max,U}}^N \approx |\Delta \mathbf{s}|_{\text{max,N}}^U \approx 0.3(a_{\text{Oberon}}/r_p)^{3/2}$ . We do not consider encounters with Jupiter, since such encounters usually result in systems that do not resemble the solar system by, e.g., ejecting the planet encountering Jupiter (Tsiganis et al. 2005).

The precession constants adopted above include the contributions from the satellites of the planets. In the case of Uranus, the contributions are mainly from Titania and Oberon. However, the nodal precession periods of Titania and Oberon ( $\gtrsim 1300$  yr due to the oblateness of Uranus alone and  $\sim 200$  yr with the inclusion of the secular interactions among the satellites; Laskar and Jacobson 1987) are much longer than the encounter timescale with either Saturn ( $r_p/v_p \sim 2$  days for  $r_p \sim a_{\text{Titan}}$ ) or Neptune ( $r_p/v_p \sim 1$  day for  $r_p \sim a_{\text{Oberon}}$ ), and their orbits would not be able to follow the equator of Uranus during the encounter (Goldreich 1965). This would reduce  $\alpha_U$  and hence

the already small maximum change in the spin direction of Uranus by a factor of 5.3. Similarly, without the contributions from the satellites to the precession constants, the maximum changes in the spin directions of Neptune and Saturn are reduced by a factor of 5.7 and 3.7, respectively. Then the maximum change in the spin direction is  $\lesssim 1^\circ$  for any pair-wise encounter among Saturn, Uranus, and Neptune, even if we consider an extremely close encounter with  $r_p$  equal to twice the sum of the planetary radii, which the regular satellite systems are unlikely to survive.

We have just shown that the change in the spin direction in *inertial space* during an encounter between the planets is very small. Thus any change in the obliquity (which is defined as the angle between the spin axis and the orbit normal) must be due to a change in the orbital inclination. As we shall see in, e.g., Figs. 1 and 2, the orbital inclinations of the ice giants can reach maximum values of  $\sim 10^\circ$ – $15^\circ$  during the encounter phase. However, because the timescale on which the inclination is changed by encounters and damped by planetesimals ( $\lesssim 1$  Myr) is much less than the precession period of the spin axis about the orbit normal due to solar torque ( $\gtrsim 2\pi/\alpha_U = 29$  Myr for Uranus), there is not enough time for the spin axis to precess much due to solar torque, and the spin axis does not stray far from its initial position nearly perpendicular to the initial orbital planes of the planets. Therefore, we expect the obliquities to return to small values as the inclinations are damped to their present values.

### 3. NUMERICAL SIMULATIONS

To verify the analytic argument in Section 2 and to eliminate the possibility of unexpected secular spin-orbit effects, we have performed numerical simulations of the Sun and the four giant planets using the symplectic  $N$ -body code SyMBA (Duncan et al. 1998), which we have modified to include spin evolution. For the orbital evolution, we ignore the negligible effects of the oblateness of the planets, and we use imposed migration and damping of eccentricity and inclination to model the effects of the planetesimals. Lee and Peale (2002) have described how SyMBA can be modified to include forced migration and damping of eccentricity and inclination. The unit vector  $\mathbf{s}_k$  of the spin direction of planet  $k$  is evolved according to

$$\begin{aligned} \frac{d\mathbf{s}_k}{dt} = & 2\alpha_k \left(\frac{A_k}{r_{0k}}\right)^3 (\hat{\mathbf{r}}_{0k} \cdot \mathbf{s}_k)(\hat{\mathbf{r}}_{0k} \times \mathbf{s}_k) \\ & + 2\alpha_k \sum_{j>0, j\neq k} \left(\frac{M_j}{M_0}\right) \left(\frac{A_k}{r_{jk}}\right)^3 (\hat{\mathbf{r}}_{jk} \cdot \mathbf{s}_k)(\hat{\mathbf{r}}_{jk} \times \mathbf{s}_k), \end{aligned} \quad (10)$$

where the symbols are as in Eq. (3), but with the subscript 0 for the Sun and  $j, k \neq 0$  for the planets. In Eq. (10), the first term is due to the torque from the Sun and the second term is due to the torques from the other planets. The recursively subdivided time step used by SyMBA to handle close encounters between the planets is also implemented for the spin evolution due to the planetary torques. In the Appendix, we describe in more details how SyMBA is modified to include spin evolution and the tests that were performed.

We present the results from 4 series of runs, each with 30 simulations. The simulations were performed with a time step of 0.125 yr. For the precession constants at the current orbital semimajor axes, we adopt  $\alpha_J = (0.077 \text{ Myr})^{-1}$  for Jupiter,  $\alpha_S = (0.26 \text{ Myr})^{-1}$  for Saturn,  $\alpha_{I_1} = \alpha_U = (4.6 \text{ Myr})^{-1}$  for the initially inner ice giant, and  $\alpha_{I_2} = \alpha_N = (17.6 \text{ Myr})^{-1}$  for the initially outer ice giant. These values include the contributions from the satellites (Tremaine 1991). Although the inner and outer ice giants can switch positions (see, e.g., Fig. 1), the fact that we adopt the parameters of Uranus (Neptune) for the initially inner (outer) ice giant is not important, because Uranus and Neptune have similar masses and  $\alpha_U A_U^3 \approx \alpha_N A_N^3$ . The four series of runs have the following initial conditions in common: the orbital eccentricities are  $10^{-3}$ ; both the orbit normals and the spin axes are tilted by  $10^{-3}$  radians (or  $0^\circ.057$ ) from the  $z$ -axis of the inertial frame; the mean anomalies, the arguments of perihelion, and the longitudes of the ascending nodes on the  $x$ - $y$  plane of both the orbits and the equators are random variables.

In series I, the initial orbital semimajor axes and the imposed migration and damping of eccentricity and inclination are similar to those adopted by Brunini (2006a). The initial semimajor axis of Jupiter is  $a_J = 5.45 \text{ AU}$ . The initial semimajor axis of Saturn is varied in the range 8.38–8.48 AU, whereas those of the ice giants are varied in the ranges 9.9–12 AU and 13.4–17.1 AU, while keeping the initial orbital separation of the ice giants larger than 2 AU. The imposed migration rate is

$$\dot{a}_k = \frac{\Delta a_k}{\tau} \exp(-t/\tau), \quad (11)$$

where  $\Delta a_k$  is the difference between the current semimajor axis,  $A_k$ , and the initial semimajor axis. The migration timescale  $\tau$  is varied between 1 and 10 Myr, and the total time span of a simulation is  $10\tau$ . The imposed eccentricity and inclination damping rates are

$$\dot{e}_k = -e_k/(2\tau_e), \quad \dot{i}_k = -i_k/(2\tau_i), \quad (12)$$

respectively, with  $\tau_e = \tau_i = \tau/10$ . The eccentricity and inclination dampings are applied only if the orbital distance of a planet is between just outside the initial orbit of the outer ice giant and 30 AU. Series II is similar to series I, but with  $\tau_e = \tau_i = \tau/20$ .

Series III and IV have initial orbital semimajor axes closer to those adopted by Tsiganis et al. (2005) and use a different prescription for migration and damping. The initial  $a_J = 5.45 \text{ AU}$ , and the initial semimajor axes of Saturn and the inner and outer ice giants are varied in the ranges 8.0–8.5 AU, 11–13 AU, and 13.5–17 AU, respectively, with the ice giants at least 2 AU apart. The main difference from series I and II is that the semimajor axis of the inner ice giant is about 1 AU larger. For the imposed migration, we use Eq. (11) for Jupiter and Saturn and

$$\dot{a}_k = \frac{\Delta a_k}{\tau} \left( \frac{t}{\tau} \right) \exp[-t^2/(2\tau^2)] \quad (13)$$

for the ice giants. With the inner ice giant further from Saturn initially, the migration rate in Eq. (13) ensures that the ice giants do not migrate too far by the time of the Jupiter-Saturn 2:1

resonance crossing, as seen in the simulations of Tsiganis et al. (2005). For all planets, the damping rates are

$$\dot{e}_k/e_k = -K_e|\dot{a}_k/a_k|, \quad \dot{i}_k/i_k = -K_i|\dot{a}_k/a_k|, \quad (14)$$

and they are applied at all times. This form of damping has been used to model planet-disk interactions (e.g., Lee and Peale 2002), and it has the reasonable property of tying the damping rates to the migration rate (i.e., less damping when the migration slows down). We adopt  $K_e = K_i = 10$  for series III and  $K_e = K_i = 5$  for series IV.

The fractions of cases with all four giant planets surviving on reasonable orbits are 47%, 73%, 57%, and 50% in series I–IV, respectively. They are all roughly consistent with the 67% reported by Tsiganis et al. (2005), given the small number of simulations in Tsiganis et al. (43 simulations) and in each of our series (30 simulations). The results from two typical simulations with all four giant planets surviving on reasonable orbits — one from series I and the other from series III — are shown in Figs. 1 and 2. Fig. 1 is an example where the ice giants switch positions. In each Figure, panel a shows the evolution of the orbital semimajor axes  $a$ , the perihelion distances  $q = a(1 - e)$ , and the aphelion distances  $Q = a(1 + e)$ , while panels b, c, and d show the evolution of the orbital inclinations  $i$ , the tilts of the spin axes from the  $z$ -axis of the inertial frame (which is nearly perpendicular to the initial orbital planes of the planets), and the obliquities  $\varepsilon$ , respectively. It can be seen from the correlation of the changes in panels b and d of each Figure that large changes in the obliquities of Saturn and the ice giants during close encounters are due to changes in orbital inclinations. The changes in the directions of the spin axes relative to inertial space during the encounters are minuscule (panel c). As the inclinations are damped to small values, the spin axes keep their orientations in inertial space, and the obliquities are similarly decreased. These behaviors are exactly what we expect from the analytic argument in Section 2.

For Jupiter, we note that both the obliquity and the tilt of the spin axis from the inertial  $z$ -axis increase to 1–3 degrees in Figs. 1 and 2. This could be due to secular spin-orbit coupling, because the spin precession due to solar torque is quite fast for Jupiter ( $\alpha_J = (0.077 \text{ Myr})^{-1}$ ), but a detailed examination of this process is beyond the scope of the present paper.

Among the cases with all four giant planets surviving on reasonable orbits (68 out of 120 simulations in all four series), there are only four cases where one or both of the ice giants have final obliquities greater than  $5^\circ$ , including one case where one of the ice giants (Neptune) has a final obliquity greater than  $10^\circ$  ( $\varepsilon_N = 27^\circ$ ). However, these cases involve one or two extremely close encounters between the planets (usually between Saturn and the initially inner ice giant), for which the regular satellite systems are unlikely to survive. Even if the regular satellites could survive these encounters, their orbits would not be able to follow the equators of the planets during the encounters, and the final obliquities obtained in our simulations (which include the contributions from the satellites) should be reduced by a factor of 5–6 (see Section 2) and  $< 5^\circ$  even in the most extreme case.

## 4. CONCLUSIONS

We have analyzed the evolution of the obliquities of the giant planets in the Nice model (Tsiganis et al. 2005), where the Jupiter-Saturn 2:1 resonance crossing led to close encounters among the giant planets and the orbital eccentricities and inclinations were eventually damped to their present values by the interactions with planetesimals. We presented a simple analytic argument which shows that the change in the spin direction of a planet in inertial space during an encounter between the planets is very small and that the change in the obliquity (which is measured from the orbit normal) is due to the change in the orbital inclination. Since the inclinations are changed by encounters and damped by planetesimal interactions on timescales much shorter than the timescales on which the spins precess due to solar torques, especially for Uranus and Neptune, the obliquities return to small values if they are small before the encounters. We have performed simulations using the symplectic integrator SyMBA modified to include spin evolution. The numerical results are consistent with the analytic argument leading to no significant remnant obliquities. The analytic argument provides a physical explanation as to why the numerical results reported by Brunini (2006a), which are not confirmed by later simulations by him using another numerical code (Brunini 2006b) or the simulations in this paper, are indeed incorrect.

Giant impacts in the late stages of the formation of Uranus and Neptune remain a plausible explanation for the obliquities of the ice giants, but a giant impact origin for Saturn’s obliquity is problematic because of its large mass and spin angular momentum (Lissauer and Safronov 1991; Dones and Tremaine 1993). Alternatively, the obliquities of the giant planets could be generated by any process that twists the total angular momentum vector of the solar system on a timescale of  $\sim 0.5$  Myr (Tremaine 1991). However, the similarity between Saturn’s spin-axis precession rate and the nodal regression rate of Neptune’s orbit, and the near match of Saturn’s  $27^\circ$  obliquity to that of the Cassini state 2 of the secular spin-orbit resonance, strongly argue for the capture of Saturn into the Cassini state whose obliquity increases during the dispersal of the planetesimal disk (Ward and Hamilton 2004; Hamilton and Ward 2004).

We thank H. F. Levison and K. Tsiganis for informative discussions. This research was supported in part by NASA grants NNG05GK58G and NNG06GF42G (M.H.L. and S.J.P.), NASA grant NNG04GJ11G (W.R.W.), and NSF grant PHY 99-07949 (E.P.).

### A. NUMERICAL METHODS

In this appendix we describe how the symplectic integrator SyMBA (Duncan et al. 1998) is modified to include the evolution of the spin axes according to Eq. (10) and the tests that were performed. Our algorithm differs from the Lie-Poisson integrator for rigid body dynamics by Touma and Wisdom (1994) in assuming principle axis rotation and handling close encounters.



SyMBA is based on a variant of the Wisdom and Holman (1991) method, with the gravitational  $N$ -body Hamiltonian written in terms of positions relative to the Sun and barycentric momenta, and employs a multiple time step technique to handle close encounters. The potential of the gravitational interaction between planets  $j$  and  $k$  is of the form  $-Gm_jm_k/r_{jk}$ , which we simplify as  $-1/r$  in the following discussion. In SyMBA, a set of cutoff radii  $R_1 > R_2 > \dots$  is chosen, with  $R_1$  a few times the mutual Hill radius, and the potential  $-1/r$  is decomposed into  $\sum_{\ell=0}^{\infty} V_{\ell}$ , or equivalently the force  $\mathbf{F}$  into  $\sum_{\ell=0}^{\infty} \mathbf{F}_{\ell} = -\sum_{\ell=0}^{\infty} \partial V_{\ell} / \partial \mathbf{r} = -\sum_{\ell=0}^{\infty} P_{\ell}(r) \mathbf{r} / r^3$ . The properties of the partition functions  $P_{\ell}(r)$  are such that (i)  $P_{\ell}$  (except  $P_0$ ) increases smoothly from zero at  $r < R_{\ell+2}$  to one at  $r = R_{\ell+1}$  and then decreases smoothly to zero at  $r \geq R_{\ell}$  and (ii)  $P_0$  increases smoothly from zero at  $r < R_2$  to one at  $r \geq R_1$ . The force  $\mathbf{F}_{\ell}$  is to be applied with a time step  $h_{\ell}$ , with  $h_{\ell}/h_{\ell+1}$  an integer ( $= 3$  in the standard implementation). A single step of overall time step  $h_0$  of the SyMBA algorithm can be represented by the following sequence of substeps:

$$E_{\text{Sun}} \left( \frac{h_0}{2} \right) E_{\text{int},0} \left( \frac{h_0}{2} \right) E_{\text{recur}}(h_0) E_{\text{int},0} \left( \frac{h_0}{2} \right) E_{\text{Sun}} \left( \frac{h_0}{2} \right). \quad (\text{A1})$$

In the substep  $E_{\text{Sun}}(h_0/2)$ , each planet takes a linear drift in its heliocentric position (corresponding to a linear drift in the position of the Sun from the barycenter) for time  $h_0/2$ . In the substep  $E_{\text{int},0}(h_0/2)$ , each planet receives a kick to its linear momentum due to the  $\ell = 0$  level forces from the other planets for time  $h_0/2$ . In the recursive substep  $E_{\text{recur}}(h_0)$ , a planet that is not having close encounters (i.e., a planet whose separation from any other planet is greater than  $R_1$ ) evolves along a Kepler orbit for time  $h_0$ , while a pair of planets having an encounter have their time steps recursively subdivided to a maximum level of  $\ell_{\text{max}}$  — with the force at level  $\ell$ ,  $\mathbf{F}_{\ell}$ , applied with a time step  $h_{\ell}$  — if their separation  $r > R_{\ell_{\text{max}}+1}$  during the overall step (see Duncan et al. 1998 for details).

In Eq. (10), the torque on the spin axis of planet  $k$  from planet  $j$  is of the form  $2\alpha_k(M_j/M_0) \times (A_k/r_{jk})^3(\hat{\mathbf{r}}_{jk} \cdot \mathbf{s}_k)(\hat{\mathbf{r}}_{jk} \times \mathbf{s}_k)$ , which we simplify as  $\mathbf{T} = r^{-3}(\hat{\mathbf{r}} \cdot \mathbf{s})(\hat{\mathbf{r}} \times \mathbf{s})$  in this discussion. As for the force  $\mathbf{F}$ , we decompose  $\mathbf{T}$  into  $\sum_{\ell=0}^{\infty} \mathbf{T}_{\ell} = \sum_{\ell=0}^{\infty} P_{\ell}(r)r^{-3}(\hat{\mathbf{r}} \cdot \mathbf{s})(\hat{\mathbf{r}} \times \mathbf{s})$  using the partition functions  $P_{\ell}(r)$ , and  $\mathbf{T}_{\ell}$  is to be applied with a time step  $h_{\ell}$ . Thus our modified algorithm (with imposed migration and damping) can be represented by the following sequence of substeps:

$$E_a \left( \frac{h_0}{2} \right) E_{ei} \left( \frac{h_0}{2} \right) E_{\text{Sun}} \left( \frac{h_0}{2} \right) E_{\text{Sun}}^{\text{spin}} \left( \frac{h_0}{2} \right) E'_{\text{int},0} \left( \frac{h_0}{2} \right) E'_{\text{recur}}(h_0) \\ E'_{\text{int},0} \left( \frac{h_0}{2} \right) E_{\text{Sun}}^{\text{spin}} \left( \frac{h_0}{2} \right) E_{\text{Sun}} \left( \frac{h_0}{2} \right) E_{ei} \left( \frac{h_0}{2} \right) E_a \left( \frac{h_0}{2} \right). \quad (\text{A2})$$

In the substep  $E_a(h_0/2)$ , the orbital semimajor axis  $a$  of each planet is changed according to the exact solution to the imposed migration rate (with all of the other orbital elements fixed) for time  $h_0/2$  (see Lee and Peale 2002 for details). Similarly, the orbital eccentricity  $e$  and inclination  $i$  of each planet are changed according to the exact solutions to the imposed damping rates for time  $h_0/2$  in the substep  $E_{ei}(h_0/2)$ . In the substep  $E_{\text{Sun}}^{\text{spin}}(h_0/2)$ , the spin of each planet is evolved due to the solar torque (i.e., the first term in Eq. (10)) alone for time  $h_0/2$ , which is a rotation of

$\mathbf{s}_k$  by an angle  $2\alpha_k(A_k/r_{0k})^3(\hat{\mathbf{r}}_{0k} \cdot \mathbf{s}_k)h_0/2$  about  $\mathbf{r}_{0k}$ , because  $\mathbf{r}_{0k}$  is fixed during this substep. The substep  $E'_{\text{int},0}(h_0/2)$  is the same as  $E_{\text{int},0}(h_0/2)$  in the original SyMBA algorithm, but it also evolves the spin direction of each planet due to the  $\ell = 0$  level torques from the other planets for time  $h_0/2$ . Unlike the substep applying the solar torque alone, there is not an exact solution for the change in the spin direction with the torques from multiple planets, and we use the midpoint method. Similarly,  $E'_{\text{recur}}(h_0)$  is the same as  $E_{\text{recur}}(h_0)$ , but it also applies the torque at level  $\ell$ ,  $\mathbf{T}_\ell$ , with a time step  $h_\ell$ , recursively down to the maximum level  $\ell_{\text{max}}$ , for a pair of planets having an encounter.

We have tested our implementation of the spin evolution with several tests. In the first set of tests, we checked that the code produces the correct spin axis precession around the orbit normal in the presence of the solar torque alone. We integrated Jupiter alone with a variety of orbital eccentricity  $e$  (up to 0.2). We also integrated the four giant planets with their current  $e$  and  $i$ , but with their masses reduced by a factor of  $10^{-10}$  (so that they are on unperturbed Kepler orbits). A variety of obliquities  $\varepsilon$  were used, and we integrated for  $10^7$  yr using a time step of 0.25 yr. We found a small variation in  $\varepsilon$  (up to  $\sim 10^{-3}$  degrees) over the period of an orbit, which is expected since Eq. (10) is not orbit-averaged, but there was no detectable secular change in  $\varepsilon$ . The average spin precession rate (measured by the total change in the longitude of the ascending node of the equator on the orbital plane) agreed with the analytic result  $\alpha(1 - e^2)^{-3/2} \cos \varepsilon$  to better than one part in  $5 \times 10^4$ .

In the second set of tests, we checked that the code produces the correct capture into (and escape from) secular spin-orbit resonance. The simulations were simplified versions of the ones in Hamilton and Ward (2004). We integrated Saturn alone with a time step of 0.58 yr. Initially,  $a = 9.54$  AU,  $e = 10^{-3}$  and  $i = 0^\circ.064$  (the last being the amplitude associated with the perturbation to Saturn’s orbital plane due to the nodal regression of Neptune). We imposed an orbital nodal precession rate of  $g = -\alpha(0.89 + 0.23e^{-t/\tau})$  (magnitude decreasing with time) or  $g = -\alpha(1.12 - 0.23e^{-t/\tau})$  (magnitude increasing with time), with  $\tau = 2.5\text{--}10 \times 10^8$  yr. In the cases where  $|g|$  was decreased from above  $\alpha$  to below  $\alpha$ , Saturn’s spin was captured into Cassini state 2, with the obliquity librating about the analytic result in Ward and Hamilton (2004). In the cases where  $|g|$  was increased from below  $\alpha$  to above  $\alpha$ , the spin was first captured into Cassini state 1, with the obliquity librating about the analytic result in Ward and Hamilton (2004). There was a jump in the obliquity when Cassini state 1 disappeared, and the obliquity subsequently oscillated about a constant value. The results agreed with the analytic theory and numerical results of Ward and Hamilton (2004) and Hamilton and Ward (2004).

As a very stringent test of the spin evolution due to close mutual planetary interactions, we performed simulations similar to the binary planet test described in Duncan et al. (1998), where two planets are in a bound orbit and their center of mass orbits a star. The center of mass of the binary was placed in a 5.2 AU circular orbit about a solar-mass star. The initial semimajor axis of the relative orbit of the binary was 0.0125 AU and the initial eccentricity was 0.4. One planet had a mass of  $M_1 = 0.9 \times 10^{-3}M_\odot$  and the other  $M_2 = 1.1 \times 10^{-3}M_\odot$ . Both planets had the

same precession constant as Jupiter, and their initial obliquities were  $\varepsilon_1 = 60^\circ$  and  $\varepsilon_2 = 30^\circ$ . We integrated this system for 500 yr (or about 16000 orbital periods of the binary). Because the torques of the planets on each other dominated over the torques from the Sun, the average precession rates of the spin axes around the normal to the relative orbit are known analytically, if we ignore the solar torques. We found that the numerical precession rates agreed with the analytic results to within 0.0008 and 0.0022 fractionally for planets 1 and 2, respectively. The small discrepancies were not sensitive to the time step (we used 0.25 yr and smaller), and they are likely real and due to solar perturbations. Solar perturbations also caused the eccentricity of the relative orbit to vary between 0.4 and 0.3964 and the obliquities to show small variations on the same timescale.

## REFERENCES

- Brunini, A., 2006a. Origin of the obliquities of the giant planets in mutual interactions in the early Solar System. *Nature* 440, 1163–1165.
- Brunini, A., 2006b. Retraction: Origin of the obliquities of the giant planets in mutual interactions in the early Solar System. *Nature* 443, 1013.
- Chiang, E., Lithwick, Y., Murray-Clay, R., Buie, M., Grundy, W., Holman, M., 2006. A brief history of trans-Neptunian space. In: Reipurth, B., Jewitt, D., Keil, K. (Eds.), *Protostars and Planets V*. Univ. of Arizona Press, Tucson, In press.
- Dones, L., Tremaine, S., 1993. On the origin of planetary spins. *Icarus* 103, 67–92.
- Duncan, M. J., Levison, H. F., Lee, M. H., 1998. A multiple time step symplectic algorithm for integrating close encounters. *Astron. J.* 116, 2067–2077.
- Goldreich, P., 1965. Inclination of satellite orbits about an oblate precessing planet. *Astron. J.* 70, 5–9.
- Goldreich, P., Lithwick, Y., Sari, R., 2004. Planet formation by coagulation: A focus on Uranus and Neptune. *Ann. Rev. Astron. Astrophys.* 42, 549–601.
- Hamilton, D. P., Ward, W. R., 2004. Tilting Saturn. II. Numerical model. *Astron. J.* 128, 2510–2517.
- Laskar, J., Jacobson, R. A., 1987. GUST86. An analytical ephemeris of the Uranian satellites. *Astron. Astrophys.* 188, 212–224.
- Lee, M. H., Peale, S. J., 2002. Dynamics and origin of the 2:1 orbital resonances of the GJ 876 planets. *Astrophys. J.* 567, 596–609.
- Lee, M. H., Peale, S. J., Pfahl, E., Ward, W. R., 2006. Evolution of the obliquities of the giant planets during migration. *Bull. Am. Astron. Soc.* 38, 611.

Lissauer, J. J., Safronov, V. S., 1991. The random component of planetary rotation. *Icarus* 93, 288–297.

Touma, J., Wisdom, J., 1994. Lie-Poisson integrators for rigid body dynamics in the solar system. *Astron. J.* 107, 1189–1202.

Tremaine, S., 1991. On the origin of the obliquities of the outer planets. *Icarus* 89, 85–92.

Tsiganis, K., Gomes, R., Morbidelli, A., Levison, H. F., 2005. Origin of the orbital architecture of the giant planets of the Solar System. *Nature* 435, 459–461.

Ward, W. R., Hamilton, D. P., 2004. Tilting Saturn. I. Analytic model. *Astron. J.* 128, 2501–2509.

Wisdom, J., Holman, M., 1991. Symplectic maps for the n-body problem. *Astron. J.* 102, 1528–1538.

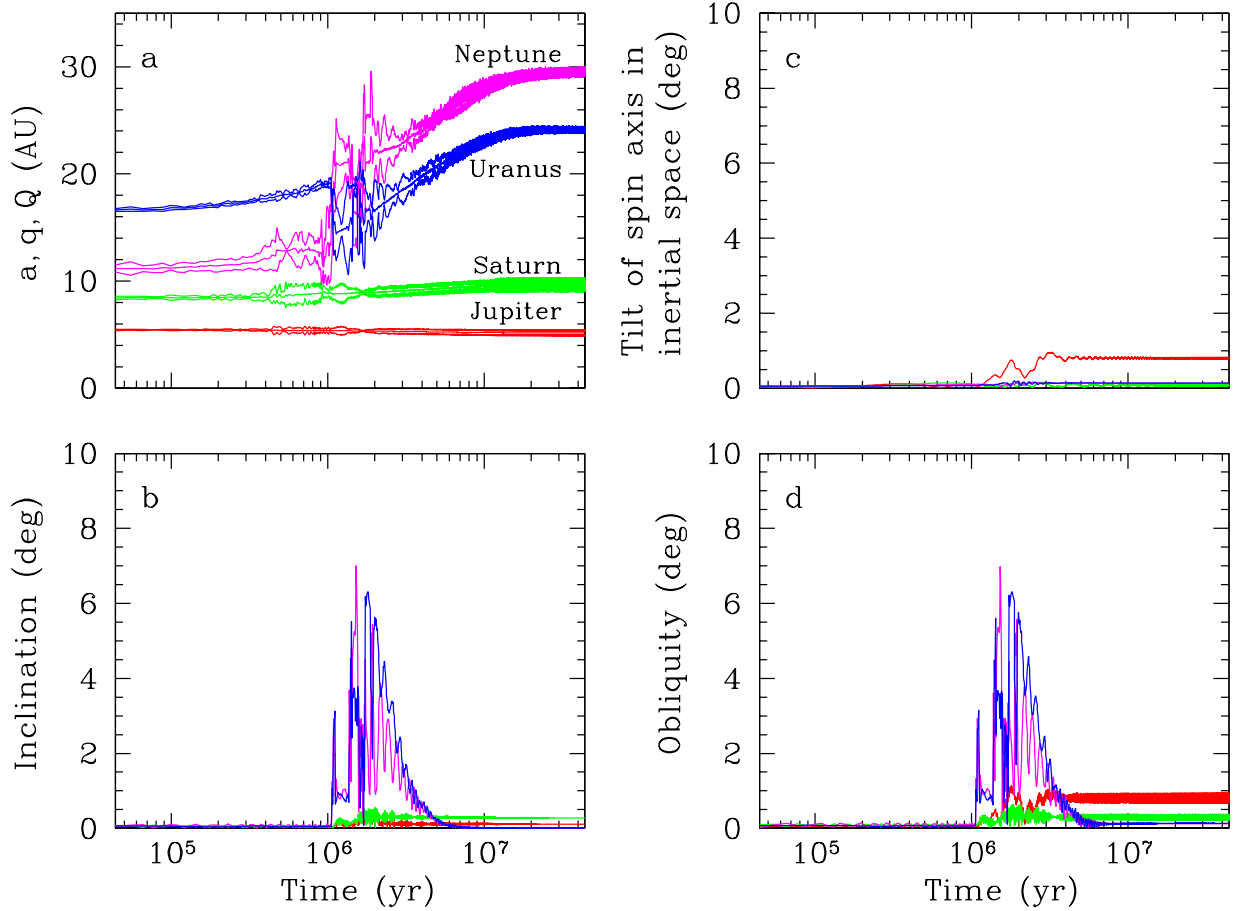


Fig. 1.— Evolution of the orbits and spin axes of the giant planets in a simulation from series I (see text for the details of the setup). (a) Orbital semimajor axis ( $a$ ) and the minimum ( $q$ ) and maximum ( $Q$ ) heliocentric distances. Note that the ice giants switch positions in this simulation. (b) Orbital inclination. (c) Tilt of the spin axis in inertial space. (d) Obliquity. The planets are Jupiter (red), Saturn (green), Uranus (blue), and Neptune (magenta). The orbital inclination and the tilt of the spin axis in inertial space are measured relative to the  $z$ -axis of the inertial frame, which is nearly perpendicular to the initial orbital planes of the planets, while the obliquity is the angle between the spin axis and the orbit normal. The directions of the spin axes show very little change in inertial space. The obliquities reflect primarily the inclinations and return to small values as the inclinations are damped.

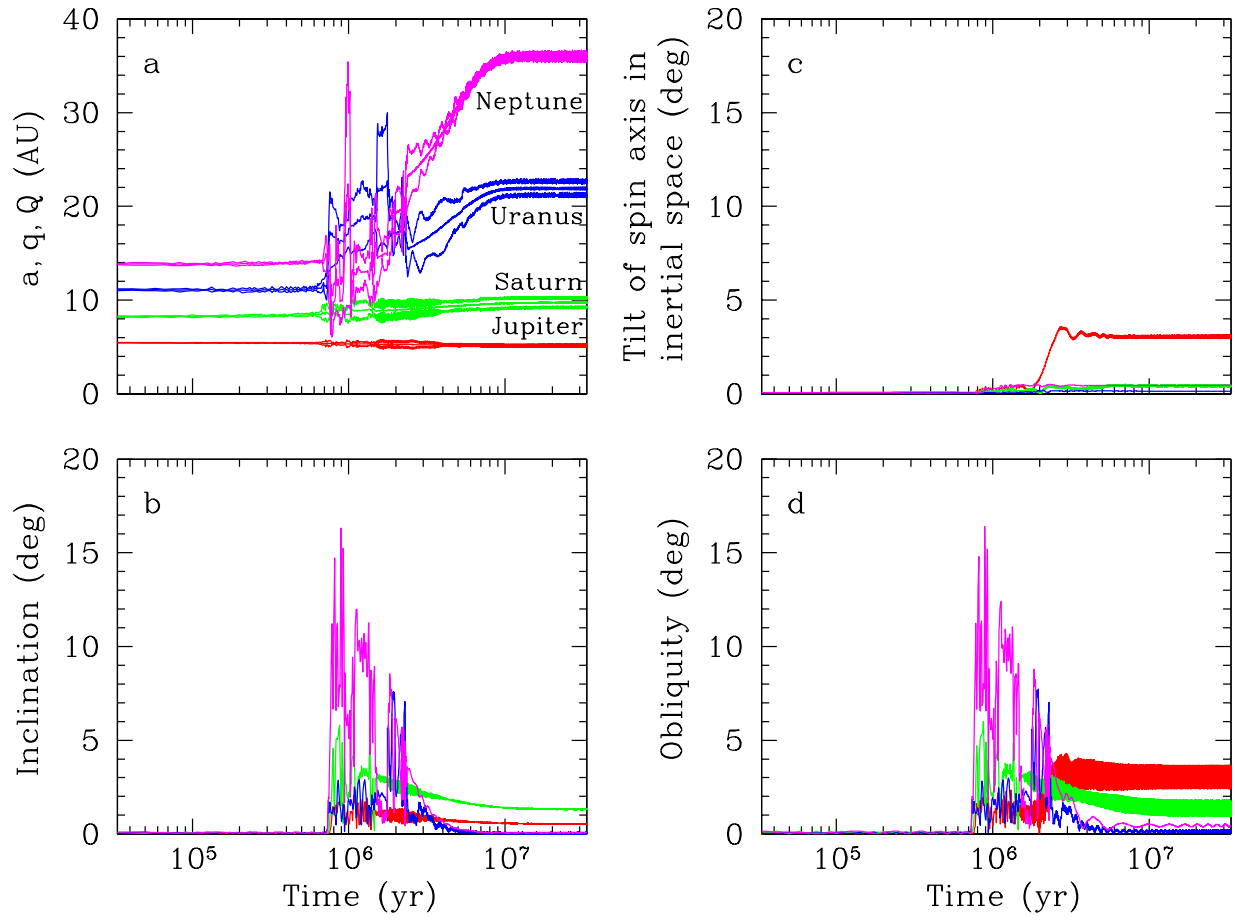


Fig. 2.— Same as Fig. 1, but for a simulation from series III. The ice giants do not switch positions in this simulation.